International Journal of Robotics and Control Systems
Vol. 3, No. 4, 2023, pp. 880-898
ISSN 2775-2658
http://pubs2.ascee.org/index.php/ijrcs

# Comparison between Compensated and Uncompensated PD with Cascade Controller Design of PMDC Motor: Real Experiments

Sopheak Yean [a,1,*], Sarot Srang [a,2]

[a] Dynamics and Control Laboratory, MIT Research Unit, Institute of Technology of Cambodia, Phnom Penh, Cambodia
[1] sopheak.yean@gsc.itc.edu.kh; [2] srangsarot@itc.edu.kh
* Corresponding Author

ARTICLE INFO

**Article history**
Received October 04, 2023
Revised November 07, 2023
Accepted November 16, 2023

**Keywords**
DC Motor;
PD Controller;
Cascade Controller;
Root Locus;
UKF

ABSTRACT

In this paper, we compare two different kinds of position controllers, namely PD (both compensated and uncompensated PD) and Cascade controller (both compensated and uncompensated Cascade). SIMULINK software is used to implement lumped parameters estimation with UKF. The Proportional-Derivative (PD) controller design by root locus and Cascade controller design have been chosen for our feedback system, and coulomb friction as disturbance is taken into account in the estimation model. The aim of this paper is to find out which controller is better (both compensated and uncompensated PD controller vs. both compensated and uncompensated Cascade controller). Therefore, the objective is to show how useful the parameter estimation for controller design with compensation. Through comparing two position controller designs, the experiment results show that both Compensated Proportional Derivative (PD) controller and Cascade controller Design have much better performance than the Uncompensated ones.



## 1. Introduction

DC motors have wide applications in industrial control system (mechatronics system, robotics and low to medium power machine tools) because they are easy to model and control. The PMDC machines have a simpler construction since the field winding of a DC motor is replaced by permanent magnet (PM). Consequently, they have become one of the most commonly used machines in many applications such as electrical vehicles, robotic manipulators, trams, or motion-controlled devices, etc [1]-[11]. Each low-cost PMDC motor produced may have different dynamical and electrical properties such as back electromotive force and torque constant, rotor resistance, friction coefficients.

As stated in [12]-[14], over the year, several methods are used to estimate these unknown parameters of DC motors such as hybrid equivalent circuit model, step response, dynamic load variation, closed-loop error approach, least-square parametric estimation, least-squares approximation technique, and a closed-loop disturbance observer. Some of the mentioned methods may need applying a varying voltage to the motor and recording the motor data shown on the measuring equipment before calculating the unknown parameters by comparing motor data with the model equation of the motor. One obstacle of using this method is the need to have third-party measuring equipment for recording data which demands high cost.

There is a large number of parameter identification methods, namely: the algebraic identification methods, the recursive least square method, the inverse theory, the least square method, the moments method [15]-[21]. When applying to DC motor parameter identification, these methods work so well for steady state response, but only some parameters can be identified. The first difficulty with these methods is to conduct many experiments at different steady state responses. Another difficulty is that in order to get all parameters for complete modeling, there needs to be distinct experiment setup to conduct for obtaining transient responses. The last disadvantage of these methods is that they require 3 measurements such as voltage, current, and angular velocity. For our method, only angular velocity measurement is needed. That thanks to the simplification technique. Furthermore, we can estimate all the lumped parameters with one-go experiment.

For control method, there are as follows: Proportional-Integral (PI), Proportional-Integral-Derivative (PID) or bipositional, Continuous PID Control Design Method, A state-space Control Design Method, Discrete PID Control Design Method [22]-[25]. The most popular among them is the PID controller since it is quite simple and easy to be implemented in a real hardware system [26]. However, in [27] the PID controller also has some weaknesses. Any slightest change in setpoint will affect the whole system's performance, and it is very hard to tune the parameters for PID controller. With our simplified model, simpler controller like PD is very suitable.

As implemented in [28]-[38], the hybrid unscented Kalman filter is used to estimate the effect of Stribeck + viscous friction of a DC motor. The estimated parameters compensate to the controller of the motor. The findings reveal that the system with friction compensation shows much better performance. It shows that by using one or another variance of the Kalman filter, it is possible to effectively estimate the unknown parameters of the DC motor. In this paper, all of the parameters are lumped, and we choose Unscented Kalman Filter for parameter estimation because the state-parameter model of the dynamic is nonlinear.

We have seen numerous previous researches comparing only two types of controllers but they never subdivide them into subtypes—compensated and uncompensated respectively. Therefore, our research problem is to investigate the different outcomes between PD controller (compensated and uncompensated) and Cascade controller (compensated and uncompensated). The results will help us conclude which control architecture is superior to the others.

This paper is structured as follows: Section 2 presents the dynamics modeling, controller design and describes the obtained UKF algorithm for parameters estimation. Section 3 presents the experiment results, discussion and conclusion are stated in section 4.

## 2. Method

### 2.1. Model DC Motor

The following DC motor model and controller design are derived based on the work as seen in [15], [16], [39]-[44].

In Fig. 1 both the back EMF (electromotive-force voltage) and the electromagnetic torque depend direct in proportionality with speed and current:

$$T_a = K_t i_a \tag{1}$$

$$V_b = K_b \omega \tag{2}$$

where $K_t$ is torque constant and $K_b$ is back EMF constant. Electromagnetic theory and classical mechanics form the basis for the development of electromechanical system models. The differential equation of the armature circuit is

$$V_a = L_a \frac{di_a}{dt} + R_a i_a + V_b \ . \tag{3}$$

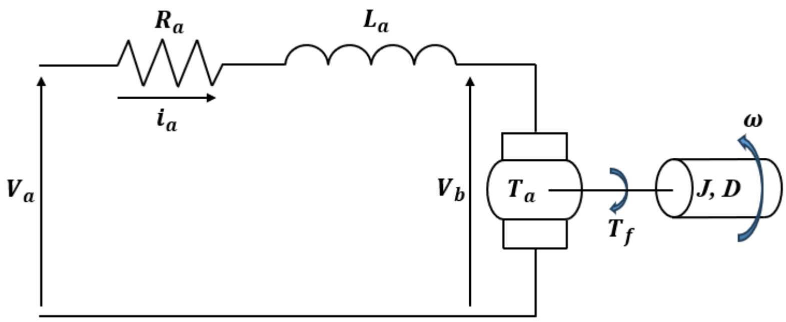


**Fig. 1.** The schematic of permanent magnet DC motor

In many practices of PMDC motor, the inductance $L_a$ in the armature circuit is very small which cause the dynamic response of the electrical part to be much faster than that of mechanical part (usually 100 to 1000 times faster). Therefore, only the dynamic of the mechanical part is of importance. Once inductance is ignored ($L_a \approx 0$), then (3) becomes

$$V_a = R_a i_a + V_b \tag{4}$$

Application of Newton's second law of motion yields the torque balance equation

$$J\dot{\omega}(t) + T_f = T_a \tag{5}$$

where $T_f$ friction torque effected by Coulomb friction $T_d$ and viscous friction $D\omega(t)$. Then the friction torque is modeled as

$$T_f = T_d sign[\omega(t)] + D\omega(t). \tag{6}$$

Substituting (6) into (5) yields

$$J\dot{\omega}(t) + T_d sign[\omega(t)] + D\omega(t) = T_a. \tag{7}$$

Using (1), (2), (4), and (7) the dynamic of the DC motor can be written as

$$\dot{\omega}(t) = -\left(\frac{R_a D + K_t K_b}{R_a J}\right)\omega(t) + \frac{K_t}{R_a J}V_a - \frac{T_d sign[\omega(t)]}{J}. \tag{8}$$

where $V_a$ is voltage applied to the armature, $R_a$ is the internal resistance of the armature, $J$ is the moment of inertia of the motor

Let $$a = \left(\frac{R_a D + K_t K_b}{R_a J}\right) \text{ and } b = \frac{K_t}{R_a J}, c = \frac{T_d}{J}.$$

Then (8) can be reduced to

$$\dot{\omega}(t) = -a\omega(t) + bV_a - c sign[\omega(t)]. \tag{9}$$

We see that the equation (9) is a nonlinear state equation for velocity model of a DC motor. The parameters $a, b,$ and $c$ of the models can be numerically estimated by using UKF. From the equation (9), we can sketch block diagram for velocity model as Fig. 2.

### 2.2. PD Controller Design by Root locus

Consider a position controller architecture with the PD controller as shown Fig. 2. The governing equation of the control system Fig. 2 can be written as

$$(\ddot{\theta}_d - \ddot{\theta}) + (bK_d + a)(\dot{\theta}_d - \dot{\theta}) + bK_d z(\theta_d - \theta) = 0. \tag{10}$$

Let the error between desired and actual position $e_\theta = \theta_d - \theta$, then $\dot{e_\theta} = \dot{\theta}_d - \dot{\theta}$ and $\ddot{e}_\theta = \ddot{\theta}_d - \ddot{\theta}$. The equation (10) can be rewritten as

$$\ddot{e}_\theta + (bK_d + a)\dot{e_\theta} + bK_d z e_\theta = 0 \tag{11}$$

Equation (11) is a second order differential equation which has characteristic solution as follow.

$$\lambda^2 + (bK_d + a)\lambda + bK_d z = 0 \tag{12}$$

Equation (12) has roots which can be real or complex numbers defined as below.

$$\lambda_1 = \frac{1}{2}\left((-a - bK_d) + \sqrt{(a - bK_d)^2 - 4bK_d z}\right)$$

$$\lambda_2 = \frac{1}{2}\left((-a - bK_d) - \sqrt{(a - bK_d)^2 - 4bK_d z}\right)$$

Let $K_p = K_d z$. The roots of (12) can be analyzed in terms of parameter as below.

When $K_d = 0$, then $\lambda_1 = 0$, and $\lambda_2 = -a$.

When $K_d \to \infty$, then from limited techniques, $\lambda_1 = -z$ and $\lambda_2 = -\infty$.

when $\Delta = \sqrt{(a - bK_d)^2 - 4bK_d z} = 0$, then (12) has double roots $\lambda_1 = \lambda_2 = \frac{1}{2}(-a - bK_d)$ and values of $K_d$ and $K_p$ are obtained as follow.

$$K_d = \frac{-a + 2z + 2\sqrt{z(z-a)}}{b} \text{ and } K_p = K_d z \tag{13}$$

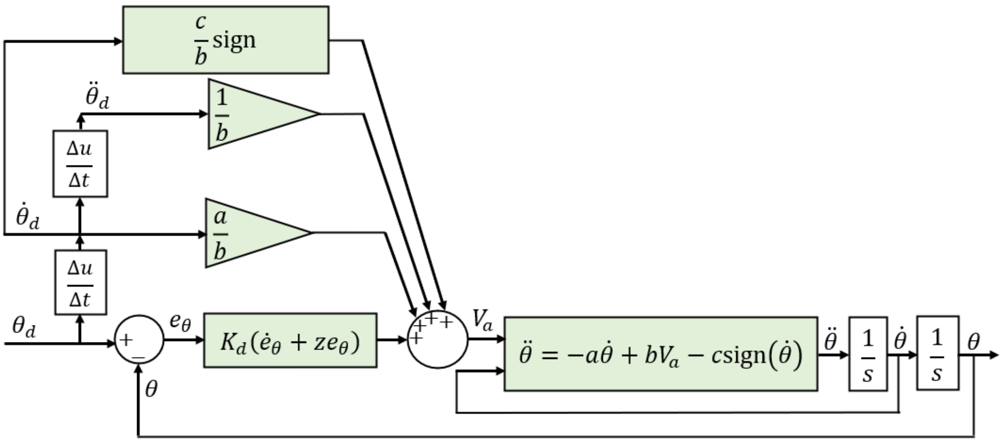


**Fig. 2.** Position control architecture with PD controller

There are two double roots (Delta $= 0$) as illustrated by root locus in Fig. 3. we choose the left double root because we prefer the critically-damped response that is the fastest one without overshoot [45].

For the friction compensation block, the velocity $\dot{\theta}$ is taken from the desired output of the motor. From root locus techniques, we can sketch a set of solutions of characteristic equations by parameter $K_d$ as in Fig. 3. Here, we see that all solution of characteristic equation is on the left side of s-plane. Hence the designed system is stable.

By selecting the value of $z$ in terms of $a$, (e.g., $z = 1.2|a| \to 1.5|a|$), proportional gain $K_p$ and derivative gain $K_d$ for the designed PD controller can be found using equation (13).

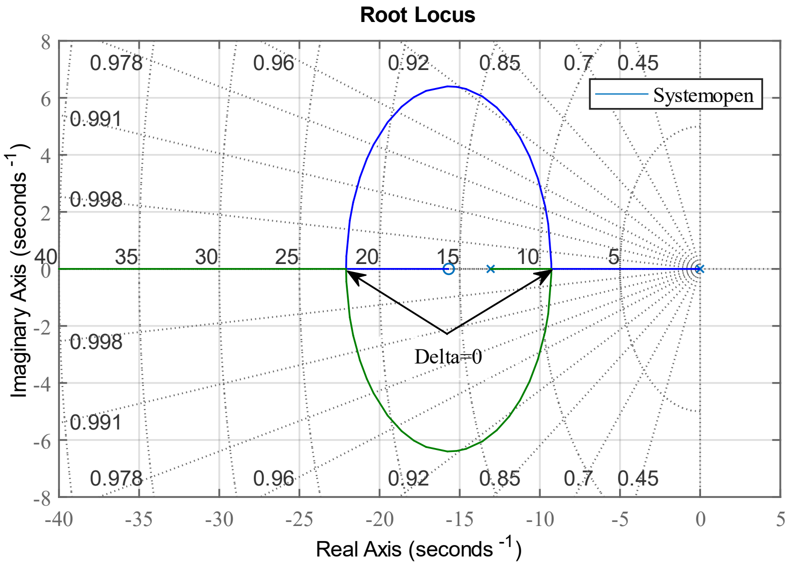


**Fig. 3.** Root locus of position control system with PD controller

### 2.3. Cascade Controller Design

Consider a position controller architecture with the Cascade controller as shown in Fig. 4. The governing equation of the control system Fig. 4 can be written as

$$\ddot{e}_\theta + (bK_d + a)\dot{e}_\theta + bK_d z e_\theta = 0 \tag{14}$$

and its characteristic form is

$$\lambda^2 + (a + bK_2)\lambda + bK_1 = 0 \tag{15}$$

Comparing (15) to the standard form of second order differential equation

$$\lambda^2 + 2\xi\omega_n\lambda + \omega_n^2 = 0 \tag{16}$$

$k_1$ and $k_2$ can be found as

$$k_1 = \frac{\omega_n^2}{b} \tag{17}$$

$$k_2 = \frac{2\xi\omega_n - a}{b} \tag{18}$$

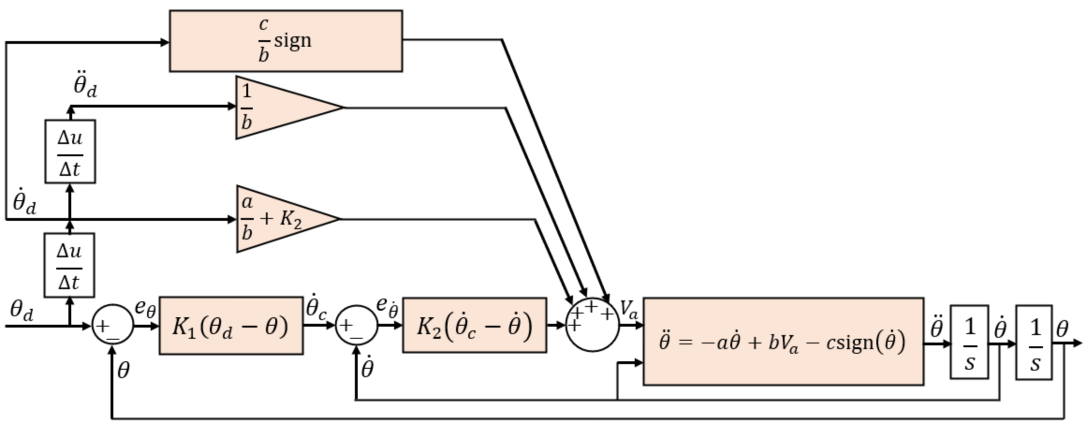


**Fig. 4.** Position control architecture with Cascade controller

### 2.4. Unscented Kalman Filter Algorithm

Unscented Kalman filter (UKF) is a variant of Kalman filter that is used to estimate state of a nonlinear dynamical system. The dynamical system is modeled as stochastic differential equation with assumption that both state dynamic and measurement are disturbed by Gaussian noises. Unlike other variants of Kalman filter that compute the state propagation and output estimation based on linear mapping function directly or obtained from linearization, UKF uses unscented transform to propagate generated sigma points via nonlinear function directly.

#### 2.4.1. Unscented Transformation

UKF consists of two steps, time update and measurement update. The proceeding step to these two is for the selection of *sigma points*. The points are taken from the source assumed to be Gaussian and map them on the target Gaussian through some nonlinear functions, and the new mean and variance of the transform are calculated. The process is called *Unscented Transformation (UT)*. The UT is presented as the following steps 1) computing set of sigma points, 2) assigning weights to each sigma point, 3) transforming the points through nonlinear function, 4) computing weighted and transformed points, 5) Computing mean and variance of the new Gaussian [46], [47].

- The selection of sigma points and weight

Sigma points generation

$$X_{[0]} = \hat{x} \tag{19}$$

$$X_{[i]} = \hat{x} + \left(\sqrt{(L+\lambda)\mathrm{P_x}}\right)_i \qquad i = 1, \dots, L \tag{20}$$

$$X_{[i]} = \hat{x} - \left(\sqrt{(L+\lambda)\mathrm{P_x}}\right)_{i-L} \qquad i = L+1, \dots, 2L \tag{21}$$

Mean contraction weights

$$W_0^{[m]} = \frac{\lambda}{(L+\lambda) + (1-\alpha^2+\beta)} \tag{22}$$

$$W_i^{[m]} = \frac{1}{2(L+\lambda)} \qquad i = 1, \dots, 2L \tag{23}$$

Covariance contraction weight

$$W_0^{[c]} = \frac{\lambda}{(L+\lambda)} \tag{24}$$

$$W_i^{[c]} = \frac{1}{2(L+\lambda)} \qquad i = 1, \dots, 2L \tag{25}$$

where $X$ is sigma points matrix with dimension $L$. $X$ has mean $\hat{x}$ and covariance matrix $\mathrm{P_x}$. $X$ is to be propagated through $Y = g(X)$. $\lambda = \alpha^2(L+k) - L$ is a scaling parameter. $\alpha$ determines the spread of the sigma points around $\hat{x}$, usually set to a small value. $k$ is a secondary scaling parameter, and $\beta$ is used to incorporate prior knowledge of the distribution of $X$. $\left(\sqrt{(L+\lambda)\mathrm{P_x}}\right)_i$ is $i$th row of the matrix square root. It is to be propagated through the nonlinear function.

- Transform sigma points through nonlinear function

$$Y_i = g\left(X_{[i]}\right) \qquad i = 0, \dots, 2L \tag{26}$$

- Mean and covariance approximation

$$\hat{y} \approx \sum_{i=0}^{2L} W_i^{[m]} Y_i \tag{27}$$

$$\mathrm{P_y} \approx \sum_{i=0}^{2L} W_i^{[c]} \{Y_i - \hat{y}\}\{Y_i - \hat{y}\}^T \tag{28}$$

where $\hat{y}$ and $\mathrm{P_y}$ are mean and covariance of $Y$ respectively. They are approximated using a weighted sample mean and covariance of the posterior sigma points.

### 2.4.2. UKF State Estimation

The UKF algorithm is provided below. The full algorithm explanation can be found in [31], [48]-[51]. In this paper, we only give a brief explanation of the algorithm. The time update and measurement update are like those of the standard Kalman filter except for the sigma points and weight calculation.

We have the state space model

$$x_{k+1} = f_d(x_k, u_k) + \sqrt{Q_d} v_k \tag{29}$$

$$y_k = h_d(x_k, u_k) + \sqrt{R} w_k \tag{30}$$

- Measurement update equations

Creating the sigma points as shown in equation (20)

$$X_{k|k-1} = [\hat{x}_{k|k-1} \quad \ldots \quad \hat{x}_{k|k-1}] + \sqrt{L+\lambda}\ [0 \quad \sqrt{P_{k|k-1}} \quad -\sqrt{P_{k|k-1}}] \tag{31}$$

The sigma points are transformed through the nonlinear function

$$Y_{k|k-1} = h_d(X_{k|k-1}, u_k) \tag{32}$$

Calculating the mean in measurement space from the propagated points

$$\hat{y}_{k|k-1} = Y_{k|k-1} w_m \tag{33}$$

where $w_m = [W_0^{(m)} \ldots\ W_{2L}^{(m)}]^T$

Calculating the covariances in measurement space

$$P_{xy,k|k-1} = X_{k|k-1}\, \overline{W} Y_{k|k-1}^T \tag{34}$$

$$P_{yy,k|k-1} = Y_{k|k-1}\, \overline{W} Y_{k|k-1}^T + R \tag{35}$$

where $\overline{W} = (I - [w_m \ldots w_m] \times \mathrm{diag}\left(\left[W_0^{(c)} \ldots\ W_{2L}^{(c)}\right]\right) \times (I - [w_m \ldots w_m])^T)$

Computing the Kalman gain

$$K_k = P_{xy,k|k-1} P_{yy,k|k-1}^{-1} \tag{36}$$

Correcting the mean and covariance

$$\hat{x}_{k|k} = \hat{x}_{k|k-1} + K_k\left(y_k - \hat{y}_{k|k-1}\right) \tag{37}$$

$$P_{k|k} = P_{k|k-1} + K_k P_{yy,k|k-1} K_k^T \tag{38}$$

- Time update equations

Creating the set of sigma points

$$X_{k|k}^{(r)} = \left[\hat{x}_{k|k} \quad \dots \quad \hat{x}_{k|k}\right] + \sqrt{L+\lambda}\left[0 \quad \sqrt{P_{k|k}} \quad -\sqrt{P_{k|k}}\right] \tag{39}$$

where $X_{k|k}^{(r)}$ is the set of resampled sigma points.

Propagating the sigma points

$$X_{k+1|k} = f_d\left(X_{k|k}^{(r)}, u_k\right) \tag{40}$$

Calculating the predicted mean and covariance

$$\hat{x}_{k+1|k} = X_{k+1|k}\, w_m \tag{41}$$

$$P_{k+1|k} = X_{k+1|k}\, \overline{W} X_{k+1|k}^T + Q_d \tag{42}$$

## 3. Experiment Results

In Fig. 5 shows the Apparatus, which was built with a low-cost PMDC motor, H-bridge driver, and Arduino Due microcontroller, is used for the experiment with hardware testing in MATLAB Simulink. The PMDC motor has gear ratio 10.2, optical encoder 100 ppr and maximum 24 voltage. The other parameters of the PMDC motor are unknown. The desired dynamic angular velocity is chosen as $V_a = 10\sin(2\pi \times 0.1t)\ (rad)$ for observation during the experiment. The desired velocity is mathematically calculated from the desired position. compensation for dynamic reference.

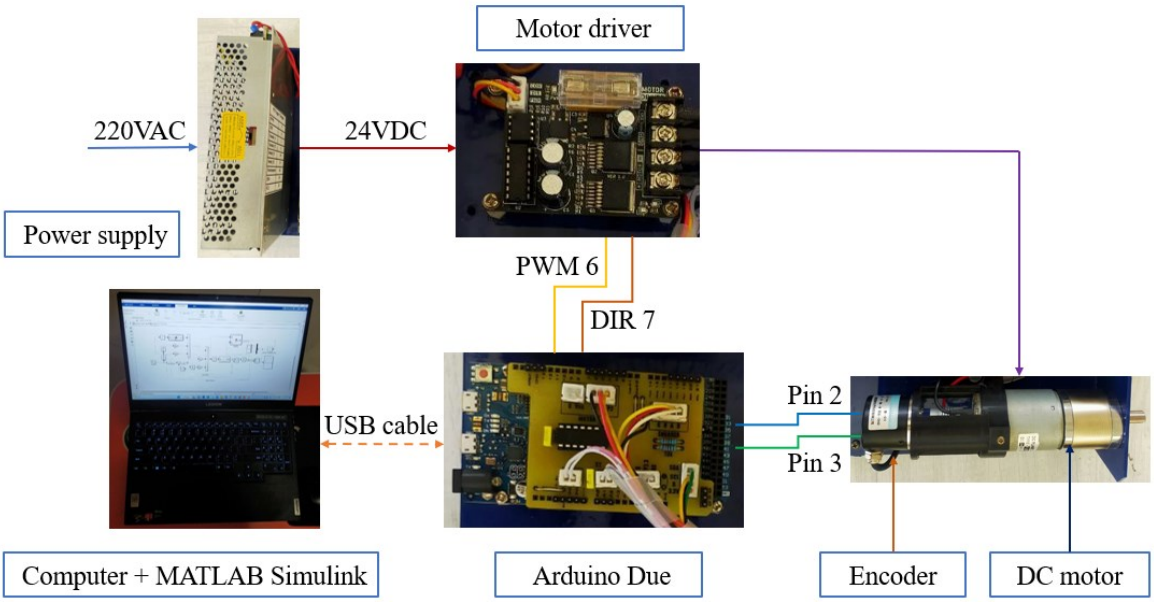


**Fig. 5.** Apparatus for experiments

The block diagram for overall system description is shown in Fig. 5. In this block, the main hardware components are implemented for this research. Arduino Due microcontroller is to control the position of DC motor by controlling the input voltage to the motor. PD and Cascade tuning algorithms is implemented in microcontroller to execute the PWM signal for DC motor drive. A 24VDC gear-motor is a powerful motor to drive the position control system. It comes with the photoelectric encoder output, planetary gear reducer and 10.2 gear ratio, which provide 100 rpm with 24VDC rated voltage. H-Bridge motor driver which is allows controlling the direction and position of DC motor.

### 3.1. UKF Implementation

We use the UKF algorithm to estimate parameters *a, b,* and *c* of the velocity model. For defining parameters as state variables, Let $x_1 = \dot{Q}_{est}$, $x_2 = a_{est}$, $x_3 = b_{est}$ , $x_4 = c_{est}$ and $x = [x_1, x_2, x_3, x_4]^T$, $T_s = 0.01s$, $Q_c = 1e-6 \times \mathrm{diag}([1; 0.1; 0.1; 0.1])$ and $R = 1e-6 \times \mathrm{diag}([2; 2])$. We performed the estimator tuning by selecting an appropriate ratio between $Q_c$ and *R*. Choosing a smaller $Q_c$ means that we have greater confidence in our model while choosing smaller *R* show greater confidence in the measurement. The velocity model (9) is rewritten as a stochastic nonlinear system as processing (State equation) and measuring (Output equation) model below.

$$\dot{x} = \begin{bmatrix} \dot{x}_1 \\ \dot{x}_2 \\ \dot{x}_3 \\ \dot{x}_4 \end{bmatrix} = \begin{bmatrix} -x_1x_2 + x_3u - x_4 sign(x_1) \\ 0 \\ 0 \\ 0 \end{bmatrix} + \sqrt{Q_c}v(t) \tag{43}$$

$$y_k = \begin{bmatrix} 1 & 0 & 0 & 0 \end{bmatrix} \begin{bmatrix} x_1 \\ x_2 \\ x_3 \\ x_4 \end{bmatrix}_k + \sqrt{R}w_k \tag{44}$$

Discretize (42) for implementing UKF algorithm, we obtain

$$x_{k+1} = \begin{bmatrix} x_1 \\ x_2 \\ x_3 \\ x_4 \end{bmatrix}_k + T_s \begin{bmatrix} -x_1x_2 + x_3u - x_4 sign(x_1) \\ 0 \\ 0 \\ 0 \end{bmatrix}_k + \sqrt{T_sQ_c}v_k \tag{45}$$

$$y_k = \begin{bmatrix} 1 & 0 & 0 & 0 \end{bmatrix} \begin{bmatrix} x_1 \\ x_2 \\ x_3 \\ x_4 \end{bmatrix}_k + \sqrt{R}w_k \tag{46}$$

### 3.2. Experiment Lumped Parameter Estimation

In Fig. 6 illustrates the model of parameter estimation for the experiment. We used input signal $V_a = 10\sin(2\pi \times 0.1t)$ $(rad)$ with velocity model in (9). The signals of the state equation and output equation are eliminated and substituted by angular velocity signal and it is fed to UKF block. The angular velocity is approximated from angular position at shaft of gearbox of DC motor as shown in Fig. 6.

Experimental results as shown in Fig. 8, Fig. 9, and Fig. 10 reveal that estimated parameter $a_{est}$, $b_{est}$ and $c_{est}$ of the DC motor converge to $12.23\,(1/\mathrm{s})$, $51.31\,(\mathrm{rad/s^2\,/\,v})$ and $27.99\,(\mathrm{Nm/kg.m^2})$ at the time of 30 second respectively with the appropriately tuned parameters of the UKF algorithm. These values are used to compensate for the feed-forward controller. We have shown that UKF could estimate the value of these parameters satisfactorily.

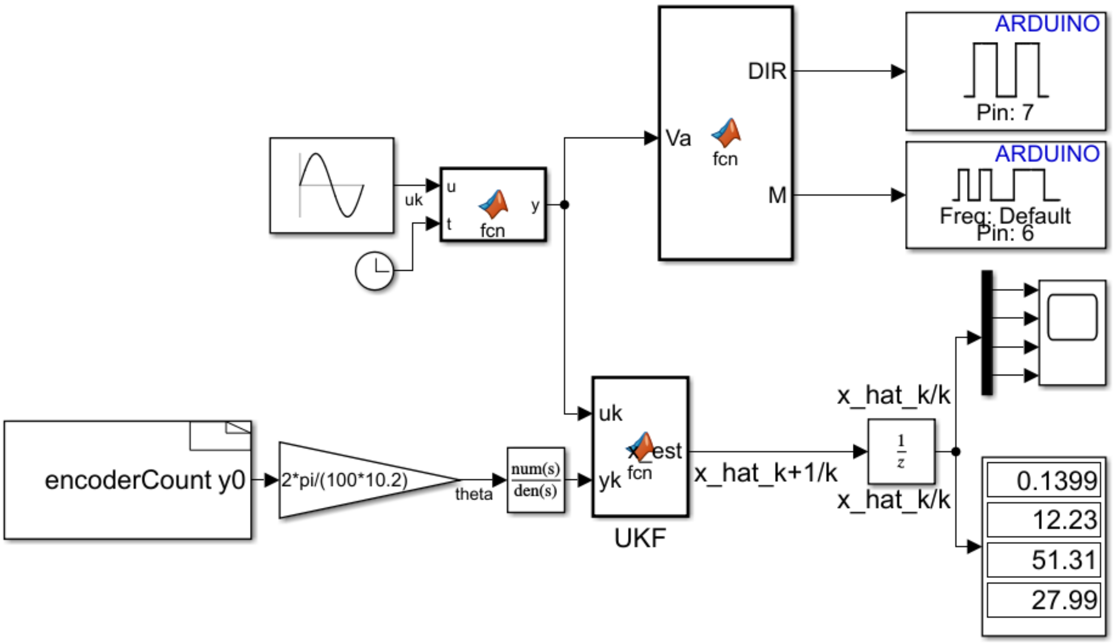


**Fig. 6.** Experiment model for estimated parameter *a, b, c*

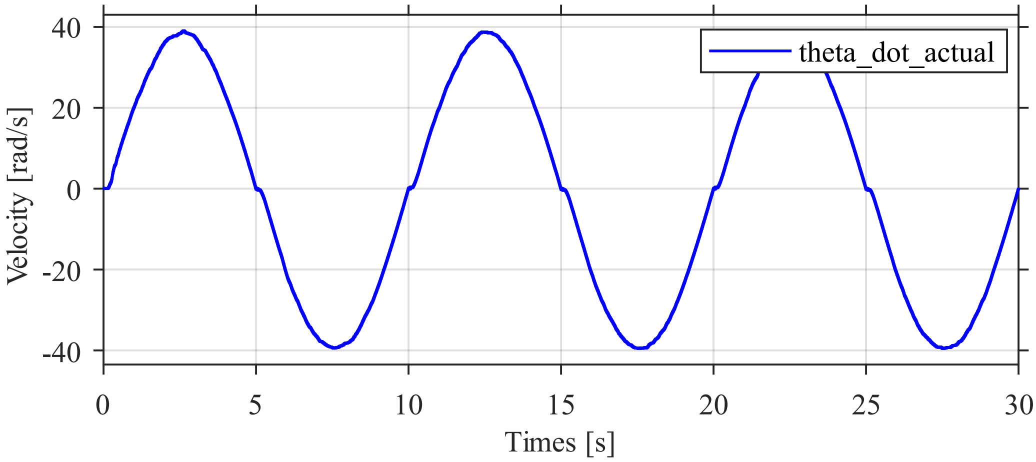


**Fig. 7.** Experiment result for velocity

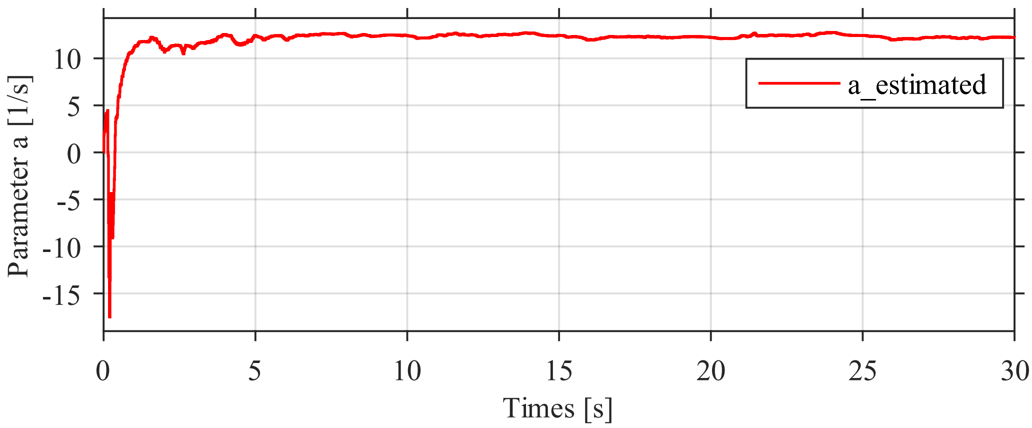


**Fig. 8.** Experiment results for estimated parameter *a*

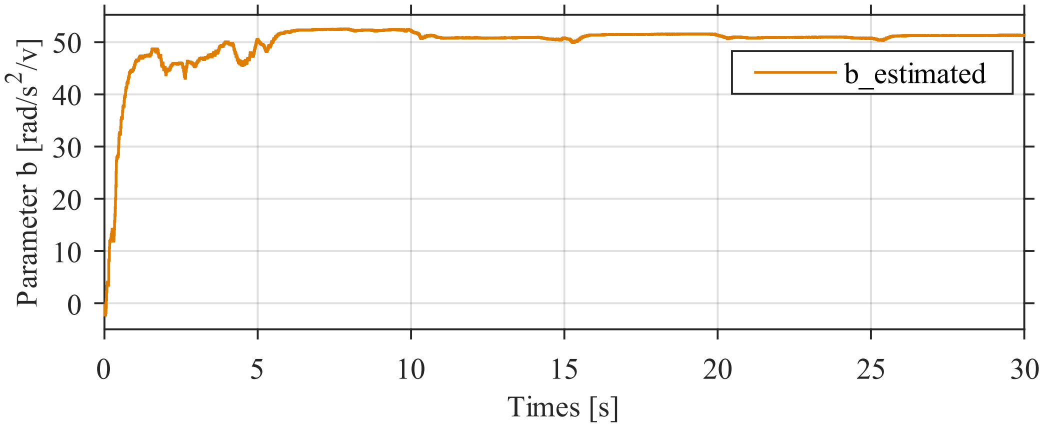


**Fig. 9.** Experiment results for estimated parameter *b*

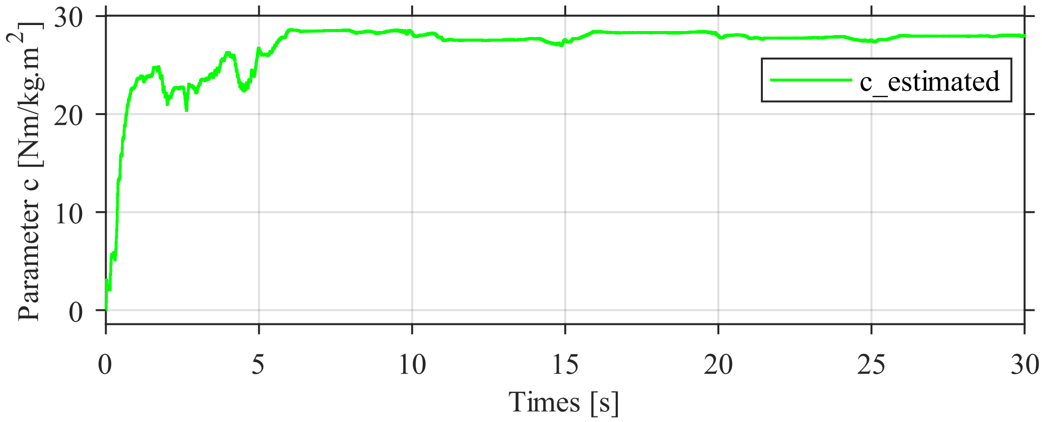


**Fig. 10.** Experiment results for estimated parameter *c*

### 3.3. Position Tracking using PD Controller

In Fig. 11 is used for experiment model in Simulink model for position control architecture with PD controller. In this real experiment, we chose lumped parameters to $a_{est} = 12.23\ (1/s)$, $b_{est} = 50.31\ (\text{rad/s}^2\ /\ \text{v})$, $c_{est} = 27.99\ (\text{Nm/kg.m}^2)$ and input signal $V_a = uk = 10\sin(2\pi * 0.1t)\ (rad)$, $T_s = 0.01\ s$. For the feed-forward ensures that the input to the motor is always regulated based on the motor's dynamic and electrical propertied.

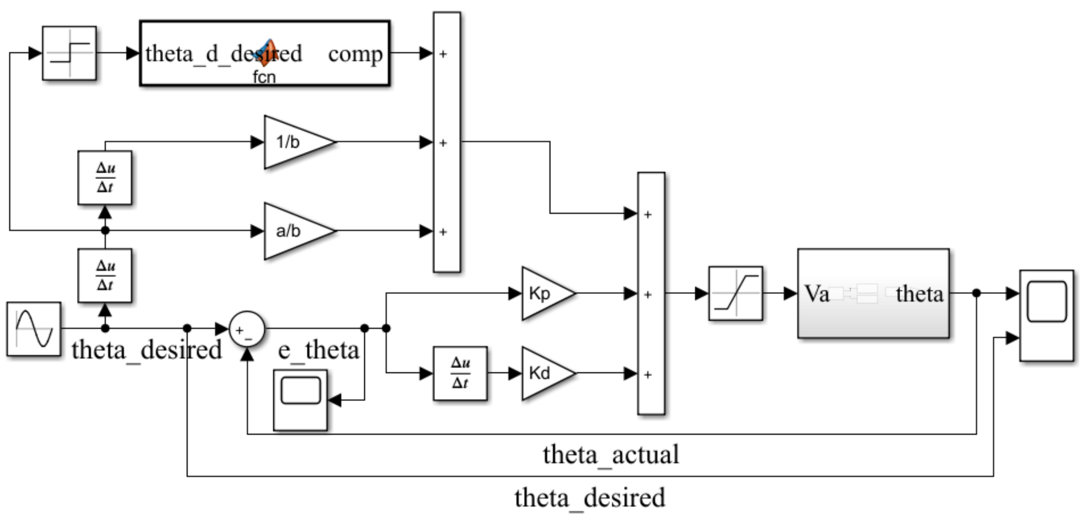


**Fig. 11.** Experiment model for position control with PD controller

In Fig. 12 shown the experiment results for position control using PD controller with friction compensation. We see that the actual position $\theta_{actual}$ is starting to converge to the desired position $\theta_d$ at a time of 2 seconds while the error values of the experiment result for error position control architecture with Compensated PD controller with the largest error within 0.028 (rad) from the actual value has shown in Fig. 14.

In Fig. 13 shown the experiment results for position control using PD controller without friction compensation. We see that the actual position $\theta_{actual}$ is starting to converge to the desired position $\theta_d$ at a time of 2 seconds while the error values of the experiment result for error position control architecture with uncompensated PD controller with the largest error within 0.24 (rad) from the actual value has shown in Fig. 15.

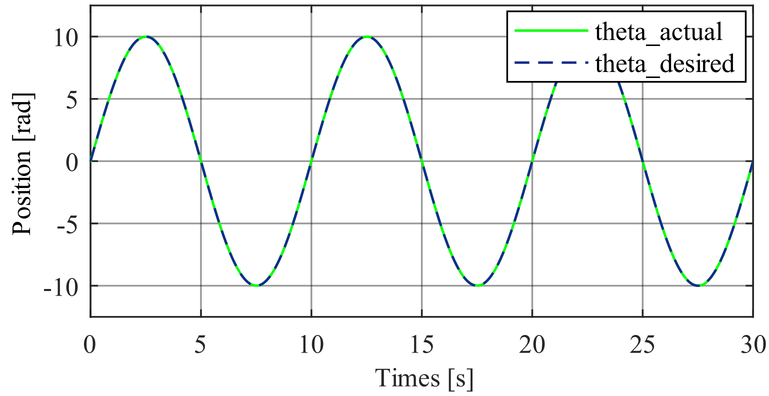


**Fig. 12.** Experiment results for desired and actual theta of PD controller with friction compensation

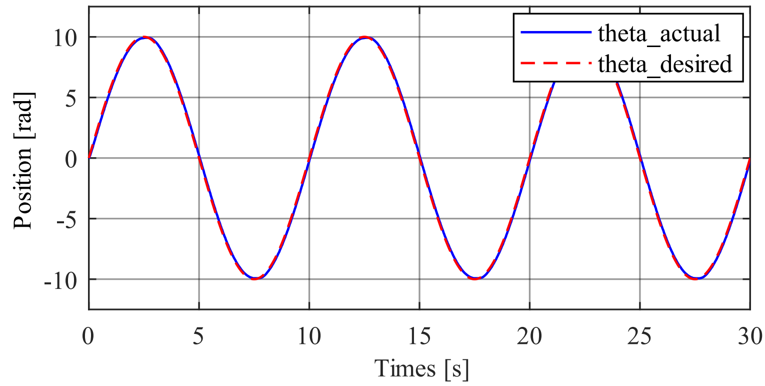


**Fig. 13.** Experiment results for desired and actual theta of PD controller without friction compensation

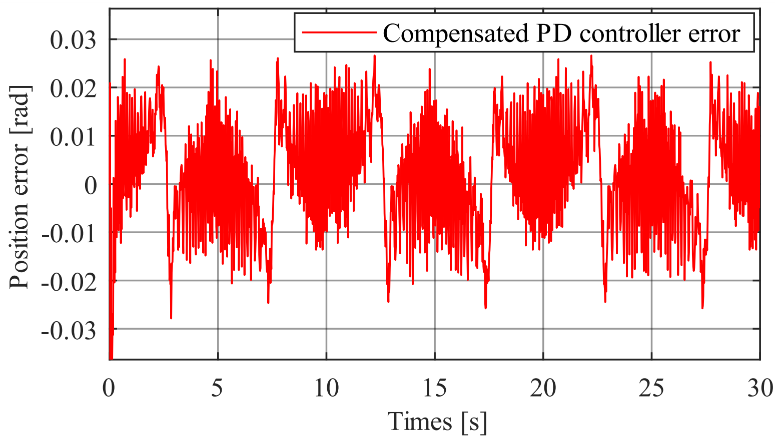


**Fig. 14.** Experiment results for position error of compensated PD controller

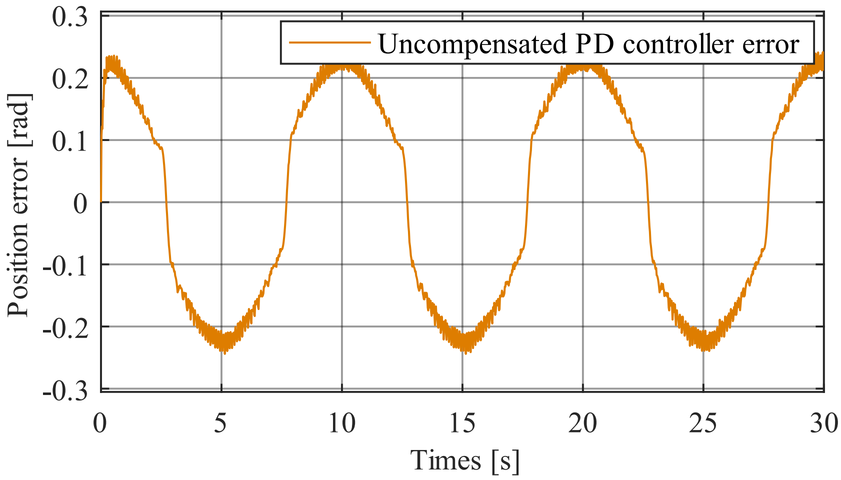


**Fig. 15.** Experiment results for position error of uncompensated PD controller

### 3.4. Position Tracking using Cascade Controller

In Fig. 16 is used for experiment model in Simulink model for position control architecture with Cascade controller. In this real experiment, we chose lumped parameters to $a_{est} = 12.23\ (1/s)$, $b_{est} = 50.31\ (\mathrm{rad/s^2\ /\ v})$, $c_{est} = 27.99\ (\mathrm{Nm/kg.m^2})$, $\zeta = 1\ \omega_n = 2 * \pi * 4,\ k_1 = \omega_n^2/b,\ k_2 = (2\xi\omega_n - a)/b$ and input signal $V_a = 10\sin(2\pi * 0.1t)\ (rad)$, $T_s = 0.01\ s$. For the feed-forward ensures that the input to the motor is always regulated based on the motor's dynamic and electrical propertied.

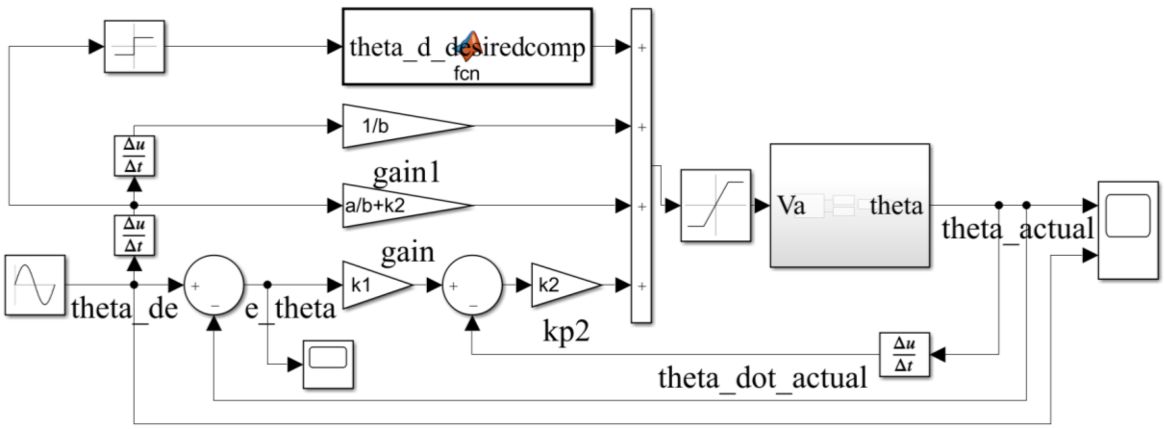


**Fig. 16.** Experiment model for position control with Cascade controller

In Fig. 17 shown the experiment results for position control using Cascade controller with friction compensation. We see that the actual position $\theta_{actual}$ is starting to converge to the desired position $\theta_d$ at a time of 2 seconds while the error values of the experiment result for error position control architecture with compensated Cascade controller with the largest error within 0.029 (rad) from the actual value has shown in Fig. 19.

In Fig. 18 shown the experiment results for position control using Cascade controller without friction compensation. We see that the actual position $\theta_{actual}$ is starting to converge to the desired position $\theta_d$ at a time of 2 seconds while the error values of the experiment result for error position control architecture with uncompensated Cascade controller with the largest error within 0.8 (rad) from the actual value has shown in Fig. 20.

In Fig. 21 shown the final experiment results of the combination of all the 4 controllers (2 compensated controllers and other 2 uncompensated controllers). We see that the dark green curve of the Uncompensated Cascade controller surges highly to 0.8 (rad) while the orange graph of the

Vol. 3, No. 4, 2023, pp. 880-898

Uncompensated PD controller rises mildly to 0.24 (rad). The two unparalleled graphs prove big errors, which is a drawback of the uncompensated controllers.

In contrast, if we take glance at the two compensated graphs (the blue and red ones), they are well-overlapped and run alongside each other. This shows that they almost have zero errors.

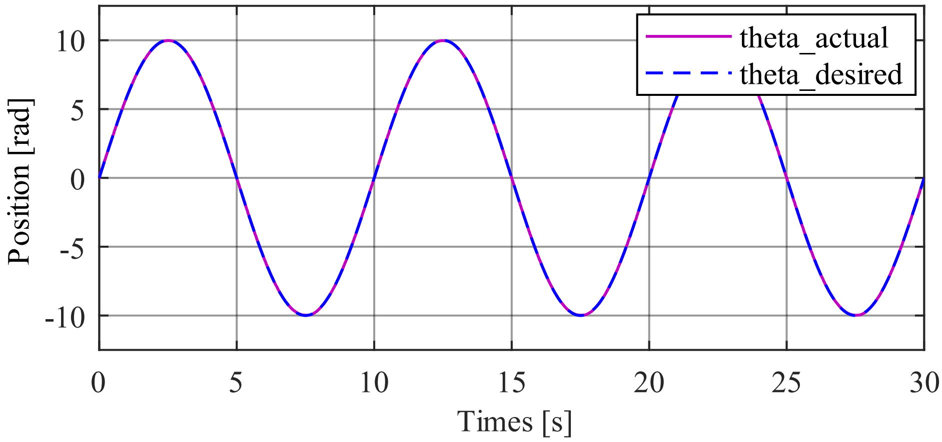


**Fig. 17.** Experiment results for desired and actual theta of Cascade controller with friction compensation

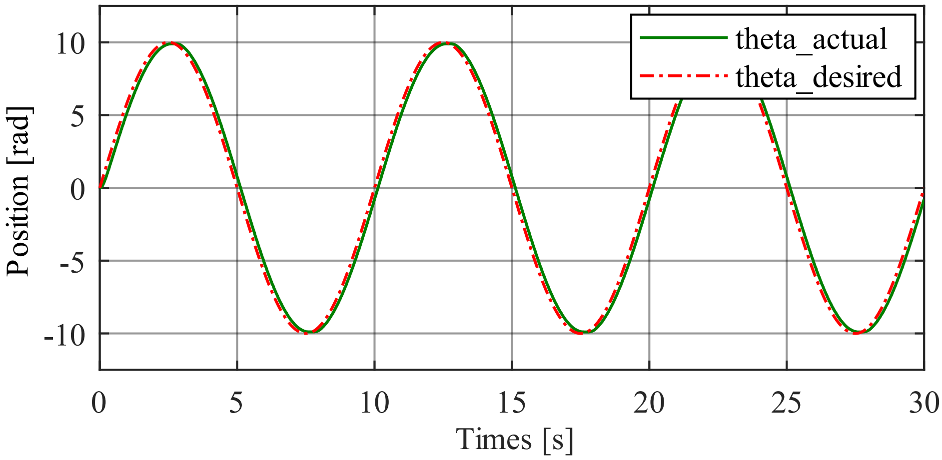


**Fig. 18.** Experiment results for desired and actual theta of Cascade controller without friction compensation

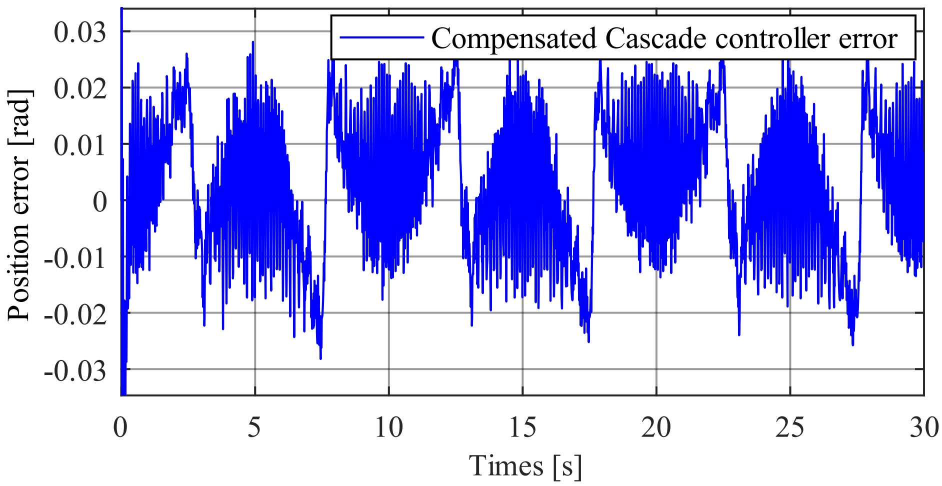


**Fig. 19.** Experiment results for Position error of compensated Cascade controller

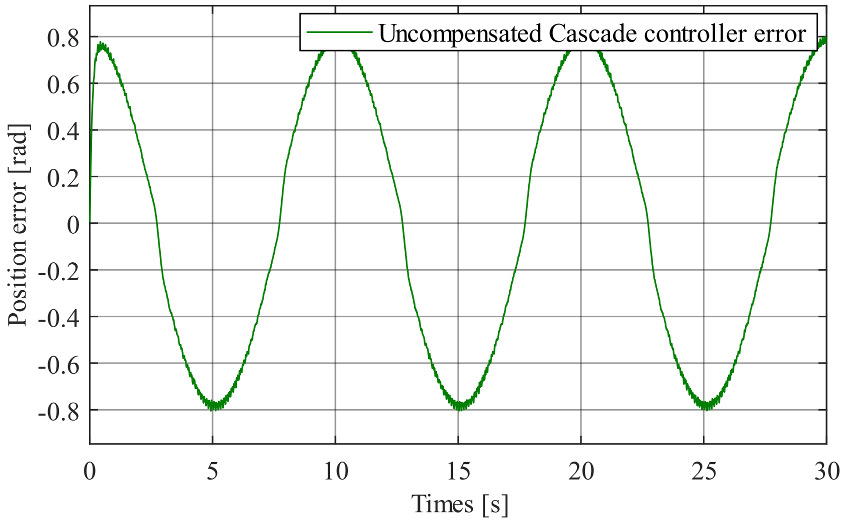


**Fig. 20.** Experiment results for position error of uncompensated Cascade controller

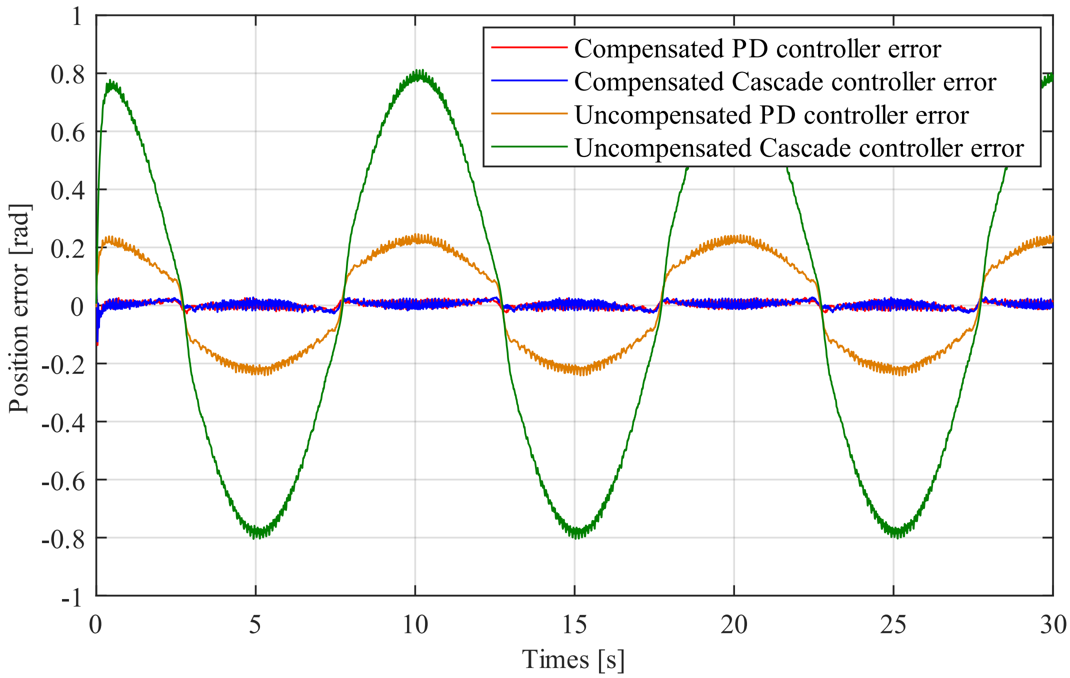


**Fig. 21.** Experiment results for position error comparison between compensated and uncompensated PD and Cascade controller

## 4. Conclusion

In this research, we derive models of a DC motor with three lumped parameters $a_{est}$, $b_{est}$, and $c_{est}$ for estimation by using UKF. To simplify the complexity of the parameter estimation, we approximate the models including the Coulomb frictional effect. Then, we use the three estimated parameters to design PD controller by root locus for position control and Cascade controller. In the parameter estimation, dynamic reference is used to capture all possible physical properties of the motor. The real experiment was conducted. Based on this experiment, the Uncompensated graphs show bigger errors than the compensated ones. In spite of trying our best to tune the Uncompensated ones, they are not still as good as the compensated ones. Therefore, the compensated controllers—either PD or Cascade—outperform the Uncompensated controllers. The maximum estimation bias of the compensated PD controller is only within 0.28% whereas that of the compensated Cascade controller is only within 0.29%. Meanwhile, the maximum estimation bias of the Uncompensated PD controller is only within 2.4% whereas that of the Uncompensated Cascade controller is only within 8%. Not knowing any parameters for compensation between both Cascade and PD controller, the expected result is not good.

One major limitation of the study is that the enterprise that produced the motor (used in this experiment) does not specify the parameters of the motor. If we know the parameters clearly, we can design controllers and apply them on mobile robots, robot arm, and UAV, etc.

In the future, we will apply that work with Online Parameter Estimation of Permanent Magnet DC Motor using an Unscented Kalman Filter.

**Author Contribution:** All authors contributed equally to the main contributor to this paper. All authors read and approved the final paper.

**Funding:** This research was funded by National Polytechnic Institute of Cambodia.

**Conflicts of Interest:** The authors declare no conflict of interest.

## References

[1] D. Saputra, A. Ma'arif, H. Maghfiroh, P. Chotikunnan, and S. N. Rahmadhia, "Design and Application of PLC-based Speed Control for DC Motor Using PID with Identification System and MATLAB Tuner," *International Journal of Robotics and Control Systems*, vol. 3, no. 2, pp. 233-244, 2023, https://doi.org/10.31763/ijrcs.v3i2.775.

[2] B. N. Kommula and V. R. Kota, "Direct instantaneous torque control of Brushless DC motor using firefly Algorithm based fractional order PID controller," *Journal of King Saud University - Engineering Sciences*, vol. 32, no. 2, pp. 133–140, Feb. 2020, https://doi.org/10.1016/j.jksues.2018.04.007.

[3] S. Srey, V. Chhour, and S. Srang, "Lumped Parameter Estimation of a Low-Cost DC Motor for Position Controller Design," *2021 International Conference on Advanced Mechatronics, Intelligent Manufacture and Industrial Automation (ICAMIMIA)*, pp. 1-6, 2021, https://doi.org/10.1109/ICAMIMIA54022.2021.9807810.

[4] H. S. Purnama, T. Sutikno, S. Alavandar, and A. C. Subrata, "Intelligent Control Strategies for Tuning PID of Speed Control of DC Motor - A Review," *2019 IEEE Conference on Energy Conversion (CENCON)*, pp. 24-30, 2019, https://doi.org/10.1109/CENCON47160.2019.8974782.

[5] J. Chotai and K. Narwekar, "Modelling and position control of brushed DC motor," *2017 International Conference on Advances in Computing, Communication and Control (ICAC3)*, pp. 1-5, 2017, https://doi.org/10.1109/ICAC3.2017.8318792.

[6] S. Devendra, B. Mahesh, K. Gaurav, and P. Gajal, "Comparison of Fuzzy-PID and PID Controller for Speed Control of DC Motor using LabVIEW," *Procedia Computer Science,* pp. 252-260, 2019, https://doi.org/10.1016/j.procs.2019.05.019.

[7] M. M. Maung, M. M. Latt, and C. M. Nwe, "DC Motor Angular Position Control using PID Controller with Friction Compensation," *International Journal of Scientific and Research Publications*, vol. 8, no. 11, pp. 149-155, 2018, http://doi.org/10.29322/IJSRP.8.11.2018.p8321.

[8] D. Handaya and R. Fauziah, "Proportional-Integral-Derivative and Linear Quadratic Regulator Control of Direct Current Motor Position using Multi-Turn Based on LabView," *Journal of Robotics and Control (JRC)*, vol. 2, no. 4, pp. 332-336, 2021, http://doi.org/10.18196/jrc.24102.

[9] A. Batool, N. Ain, A. A. Amin, M. Adnan, and M. H. Shahbaz, "A comparative study of DC servo motor parameter estimation using various techniques," *Journal for Control, Measurement, Electronics, Computing and Communications*, vol. 63, no. 2, pp. 303–312, 2022, https://doi.org/10.1080/00051144.2022.2036935.

[10] M. F. Fazdi and P-W. Hsueh, "Parameters Identification of a Permanent Magnet DC Motor: A Review," *MDPI journals*, *Electronics*, vol. 12, no. 12, 2023, https://doi.org/10.3390/electronics12122559.

[11] H. M. Usman, S. Mukhopadhyay, and H. Rehman, "Permanent magnet DC motor parameters estimation via universal adaptive stabilization," *Control Engineering Practice,* pp. 50-62, 2019, https://doi.org/10.1016/j.conengprac.2019.06.006.

[12] B. Robert, "Dynamic determination of DC motor parameters -Simulation and testing," *2014 6th IEEE International Conference on Electronics, Computers and Artificial Intelligence (ECAI)*, pp. 13–18, 2014, http://doi.org/10.1109/ECAI.2014.7090191.

[13] V. Ivan and K. Michal, "Experimental Friction Identification of a DC Motor," *International Journal of Mechanics and Applications*, pp. 26-30, 2013, http://article.sapub.org/10.5923.j.mechanics.20130301.04.html.

[14] A. Kapun, M. Čurkovič, A. Hace, and K. Jezernik, "Identifying dynamic model parameters of a BLDC motor," pp. 1254-1265, 2008, https://doi.org/10.1016/j.simpat.2008.06.003.

[15] M. Hadef and M. R. Mekideche, "Parameter identification of a separately excited dc motor via inverse problem methodology," *Turkish Journal of Electrical Engineering and Computer Sciences*, vol. 17, no. 2, pp. 99-106, 2009, https://doi.org/10.3906/elk-0805-5.

[16] M. L. Awoda and S. A. Ramzy, "Parameter Estimation of a Permanent Magnets DC motor." *Iraqi Journal for Electrical and Electronic Engineering,* vol. 15, no. 1, pp. 28–36, 2019, https://doi.org/10.37917/ijeee.15.1.3.

[17] M. Li and Y. Ma, "Parameter Identification of DC Motor based on Compound Least Square Method," *2020 IEEE 5th Information Technology and Mechatronics Engineering Conference (ITOEC)*, pp. 1107-1111, 2020, https://doi.org/10.1109/ITOEC49072.2020.9141652.

[18] D. Gao, S. Wu, J. Yu, M. Wang, and Y. Wang, "Parameter identification of DC motor model based on improved dynamic forgetting factor recursive least squares method," *2022 IEEE 8th International Conference on Smart Instrumentation, Measurement and Applications (ICSIMA)*, pp. 282-286, 2022, https://doi.org/10.1109/ICSIMA55652.2022.9929227.

[19] S. Arshad, S. Qamar, T. Jabbar, and A. Malik, "Parameter estimation of a DC motor using ordinary least squares and recursive least squares algorithms," *Proceedings of the 8th International Conference on Frontiers of Information Technology*, no. 31, pp. 1–5, 2010, https://doi.org/10.1145/1943628.1943659.

[20] J. Becedas, G. Mamani and V. Feliu, "Algebraic parameters identification of DC motors: methodology and analysis," *International Journal of Systems Science*, vol. 41, no. 10, pp. 1241-1255, 2010, https://doi.org/10.1080/00207720903244097.

[21] M. Hadef, A. Bourouina, and M. Mekideche, Parameter Identification of a DC Motor via Moments Method," *Iranian journal of electrical and computer engineering*, vol. 7, pp. 159-163, 2008, https://api.semanticscholar.org/CorpusID:112010258.

[22] W. Wu, "DC Motor Parameter Identification Using Speed Step Responses," *Modelling and Simulation in Engineering*, pp. 1–5, 2012, https://doi.org/10.1155/2012/189757.

[23] J. A. Mohammed, "Modeling, Analysis and Speed Control Design Methods of a DC Motor," *Eng. & Tech. Journal*, vol. 29, no. 1, pp. 141-155, 2011, https://api.semanticscholar.org/CorpusID:16729553.

[24] A. Khalid and A. Nawaz, "Sensor less control of DC motor using Kalman filter for low-cost CNC machine," *2014 International Conference on Robotics and Emerging Allied Technologies in Engineering (iCREATE)*, pp. 180-185, 2014, https://doi.org/10.1109/iCREATE.2014.6828362.

[25] M. Huba, S. Chamraz, P. Bistak, and D. Vrancic, "Making the PI and PID Controller Tuning Inspired by Ziegler and Nichols Precise and Reliable," pp. 2-26, 2021, https://doi.org/10.3390/s21186157.

[26] O. E Daniel and O. P Patrick, "Comparative Study Of PD, PI And PID Controllers For Control Of A Single Joint System In Robots," *The International Journal of Engineering and Science (IJES)*, pp. 51-54, 2018, https://www.theijes.com/papers/vol7-issue9/Version-2/H0709025154.pdf.

[27] A. Ma'arif and N. R. Setiawan, "Control of DC Motor Using Integral State Feedback and Comparison with PID: Simulation and Arduino Implementation," *Journal of Robotics and Control (JRC)*, vol. 2, no. 5, pp. 456-461, 2021, http://dx.doi.org/10.18196/jrc.25122

[28] S. Srang and M. Yamakita, "Adaptive Friction Compensation for a Position Control System with Stribeck Friction using Hybrid Unscented Kalman Filter," *International Journal of Information and Communication Technology*, vol. 5, pp. 283-295, 2013, https://doi.org/10.1504/IJICT.2013.054936.

[29] S. Sarkka, "On Unscented Kalman Filtering for State Estimation of Continuous-Time Nonlinear Systems," in *IEEE Transactions on Automatic Control*, vol. 52, no. 9, pp. 1631-1641, 2007, https://doi.org/10.1109/TAC.2007.904453.

[30] M. Ardeshir and R. Ahmad, "Performance evaluation of nonlinear Kalman filtering techniques in low-speed brushless DC motors driven sensor-less positioning systems," *Control Engineering Practice,* pp. 148-156, 2017, https://doi.org/10.1016/j.conengprac.2017.01.004.

[31] S. Yang and H. Li, "Application of EKF and UKF in Target Tracking Problem," *2016 8th International Conference on Intelligent Human-Machine Systems and Cybernetics (IHMSC)*, pp. 116-120, 2016, https://doi.org/10.1109/IHMSC.2016.25.

[32] P. Pichlík, "Comparison of Different Kalman Filter Types Performance for a Locomotive Slip Control Purposes," in *2017 9th International Conference on Electronics, Computers and Artificial Intelligence (ECAI)*, pp. 1-4, 2017, https://poster.fel.cvut.cz/poster2017/proceedings/Poster_2017/Section_PE/PE_005_Pichlik.pdf.

[33] M. S. Grewal and A. P. Andrews, "Applications of Kalman Filtering in Aerospace 1960 to the Present [Historical Perspectives]," in *IEEE Control Systems Magazine*, vol. 30, no. 3, pp. 69-78, 2010, https://doi.org/10.1109/MCS.2010.936465.

[34] F. Auger, M. Hilairet, J. M. Guerrero, and E. Monmasson, T. Orlowska-Kowalska and S. Katsura, "Industrial Applications of the Kalman Filter," *IEEE Transactions on Industrial Electronics*, pp. 5458–5471, 2013, https://doi.org/10.1109/TIE.2012.2236994.

[35] F. Auger, J. M. Guerrero, M. Hilairet, S. Katsura, E. Monmasson, and T. Orlowska-Kowalska, "Introduction to the Special Section on Industrial Applications and Implementation Issues of the Kalman Filter," in *IEEE Transactions on Industrial Electronics*, vol. 59, no. 11, pp. 4165-4168, 2012, https://doi.org/10.1109/TIE.2012.2194411.

[36] K. Szabat and T. Orlowska-Kowalska, "Performance Improvement of Industrial Drives With Mechanical Elasticity Using Nonlinear Adaptive Kalman Filter," in *IEEE Transactions on Industrial Electronics*, vol. 55, no. 3, pp. 1075-1084, 2008, https://doi.org/10.1109/TIE.2008.917081.

[37] E. Laroche, E. Sedda and C. Durieu, "Methodological Insights for Online Estimation of Induction Motor Parameters," in *IEEE Transactions on Control Systems Technology*, vol. 16, no. 5, pp. 1021-1028, 2008, https://doi.org/10.1109/TCST.2007.916317.

[38] S. Jafarzadeh, C. Lascu, and M. S. Fadali, "State Estimation of Induction Motor Drives Using the Unscented Kalman Filter," in *IEEE Transactions on Industrial Electronics*, vol. 59, no. 11, pp. 4207-4216, 2012, https://doi.org/10.1109/TIE.2011.2174533.

[39] M. Piao, Y. Wang, M. Sun, and Z. Chen, "Friction compensation and limit cycle suppression at low velocities based on extended state observer," *IFAC-PapersOnLine*, vol. 53, no. 2, pp. 1313-1318, 2020, https://doi.org/10.1016/j.ifacol.2020.12.1863.

[40] S. Yean, T. Peou, B. Sethy and S. Srang, "PD Controller and Dynamic Compensation Design for a DC Motor based on Estimated Parameters," *2021 International Conference on Advanced Mechatronics, Intelligent Manufacture and Industrial Automation (ICAMIMIA)*, pp. 7-12, 2021, https://doi.org/10.1109/ICAMIMIA54022.2021.9807796.

[41] M. S. Amiri, M. F. Ibrahim and R. Ramli, "Optimal parameter estimation for a DC motor using genetic algorithm," *International Journal of Power Electronics and Drive System (IJPEDS)*, vol. 11, no. 2, pp. 1047-1054, 2020, https://doi.org/10.11591/ijpeds.v11.i2.pp1047-1054.

[42] A. Ma'arif, H. Nabila, Iswanto, and O. Wahyunggoro, "Application of Intelligent Search Algorithms in Proportional-Integral-Derivative Control of Direct-Current Motor System," in *Journal of Physics: Conference Series*, vol. 1373, no. 1, pp. 1–10, 2019, https://doi.org/10.1088/1742-6596/1373/1/012039.

[43] T. N. Gücin, M. Biberoğlu, B. Fincan and M. O. Gülbahçe, "Tuning cascade PI(D) controllers in PMDC motor drives: A performance comparison for different types of tuning methods," *2015 9th International*

*Conference on Electrical and Electronics Engineering (ELECO)*, pp. 1061-1066, 2015, https://doi.org/10.1109/ELECO.2015.7394556.

[44] K. G. Abdulhussein, N. M. Yasin, and I. J. Hasan, “Comparison of cascade P-PI controller tuning methods for PMDC motor based on intelligence techniques,” *International Journal of Electrical and Computer Engineering (IJECE)*, vol. 12, no. 1, pp. 1-11, 2022, http://doi.org/10.11591/ijece.v12i1.pp1-11.

[45] N. S. Nise, “Control Systems Engineering 7th Edition,” Pomona, United States, pp. 164-169, 2015, https://www.amazon.com/Control-Systems-Engineering-Norman-Nise-ebook/dp/B00UGE1DJW.

[46] E. A. Wan and R. van Der Merwe, “The unscented Kalman filter for nonlinear estimation,” *Proceedings of the IEEE 2000 Adaptive Systems for Signal Processing, Communications, and Control Symposium (Cat. No.00EX373)*, pp. 153-158, 2000, https://doi.org/10.1109/ASSPCC.2000.882463.

[47] A. Mehrjouyan and A. Alfi, “Robust adaptive unscented Kalman filter for bearings-only tracking in three dimensional case,” *Applied Ocean Research*, vol. 87, pp. 223-232, 2019, https://doi.org/10.1016/j.apor.2019.01.034.

[48] H. B. Khamseh, S. Ghorbani, and F. Janabi-Sharifi, “Unscented Kalman filter state estimation for manipulating unmanned aerial vehicles,” *Aerospace Science and Technology*, vol. 92, pp. 446-463, 2019, https://doi.org/10.1016/j.ast.2019.06.009.

[49] E. A. Wan and R. van der Merwe, “The Unscented Kalman Filter,” *Kalman Filtering and Neural Networks*, pp. 221-280, 2001, https://doi.org/10.1002/0471221546.ch7.

[50] H. Yan, G. Huang, H. Wang, and R. Shu, “Application of Unscented Kalman Filter for Flying Target Tracking,” *2013 International Conference on Information Science and Cloud Computing*, pp. 61-66, 2013, https://doi.org/10.1109/ISCC.2013.10.

[51] P. Gu, Z. Jing, and L. Wu, “Adaptive fading factor unscented Kalman filter with application to target tracking,” *Aerospace Systems*, vol. 4, pp. 1-6, 2021, https://doi.org/10.1007/s42401-020-00071-w.